

QUALITY ASSESSMENTS OF UNMANNED AERIAL VEHICLE (UAV) AND TERRESTRIAL LASER SCANNING (TLS) METHODS IN ROAD CRACKS MAPPING

Tan Jia Yi and Anuar bin Ahmad

Department of Geoinformation, Faculty of Built Environment and Surveying
Universiti Teknologi Malaysia,
81310, Johor Bahru, Johor, Malaysia

Commission IV, WG 7

KEY WORDS: Road Cracks Mapping; Unmanned Aerial Vehicle (UAV); Terrestrial Laser Scanning (TLS)

ABSTRACT:

In general, poor road conditions, specifically road cracks constitute a public nuisance, causing troublesome to road users, severe damage to vehicles and accidents. Hence, it is essential to detect the road crack earlier as an early-stage preventive for maintenance, but traditional inspection method used in Malaysia to physically collect the road information is extremely time-consuming, hazardous and labour-intensive. Nowadays, new technologies have improved the measuring performance. This leaves a gap in comparing two modern technologies in road cracks mapping. This study aims to explore the quality assessment between the unmanned aerial vehicle (UAV) and terrestrial laser scanning (TLS) methods in road cracks mapping. Two study areas inside the campus of Universiti Teknologi Malaysia (UTM), Johor, were selected. The ground control points (GCPs) and check points (CPs) at the study areas were georeferenced by global navigation satellite system (GNSS) data with MyRTKNet and ISKnet connections. Low altitude aerial imageries were collected using DJI Phantom 4 UAV, while Topcon GLS-2000 was employed to acquire the dense data of the cracked road. GNSS and manual inspection methods were performed to evaluate the results. In terms of mapping and measurement, both TLS and UAV methods produce almost similar results with average RMSE differences ranging from ± 0.003 m to ± 0.030 m and ± 0.042 m to ± 0.224 m respectively. This revealed that TLS is more accurate than UAV in mapping and measuring work. Differences in DTM quality across these approaches is below two (2) cm. Based on this study, TLS is more reliable than UAV. However, UAV offers advantages based on several considerations such as cost, time, safety, and accessibility. In summary, findings from this study shed some light to the authorities on the feasibility of UAV and TLS methods in road cracks mapping.

1. INTRODUCTION

Over the past few decades, agencies tasked with road maintenance have found it challenging to keep them in decent condition. The road health condition in Malaysia, particularly the road cracks issue, has arisen a significant problem in road traffic and safety for the comfortable level of road users. It also adversely impacts on time delays, petrol prices, vehicle servicing fees and proves to be troublesome for all road users. This problem becomes exacerbated when maintenance is continuously neglected, resulting in rapid road deterioration and eventually contributing to road accidents (Salleh, 2016; Idris & Mohamed, 2020; Wartawan Nabalu News 2021).

Ahmad (2002) asserted that maintenance is an integral part of any structure's lifespan for its serviceability, longevity and to avoid any deterioration. Therefore, it is essential to detect the road crack earlier as an early-stage preventive for maintenance. This would effectively reduce the risk of accidents and maintenance costs. Understanding that typical road information is necessary for road maintenance and it needs to be updated to address the issues. Therefore, it is important to study road cracks detection using the effective way for timely crack repair. Road crack is a crucial indicator in pavement design where related agencies require the road condition information to plan for the road network management, cost, time, and quantity of

ingredients needed for the road repair (Staniek, 2017). Hence, a georeferenced map that evaluates and plots the road quality is essential to manage road maintenance (Miraliakbari et al., 2014). It is a well-known fact that identifying road cracks with manual procedures in an area can be a difficult endeavour when there is wrong or missing information. Data collection by inspectors to physically measure and map the road distress in order to prepare a report is extremely time-consuming, hazardous, labour-intensive and subjective. Not only does it cause traffic disruptions, but also poses a safety risk to engineers. In recent years, there has been a major evolution in the field of surveying instrumentation and led the efforts to adopt unmanned aerial vehicles (UAV) and terrestrial laser scanning (TLS) as integral technology for engineering-related works since UAV and TLS can quickly capture detailed information due to their high level of automation and performance as well as their ease of use (Yurtseven, 2019).

This study aims to explore the quality assessment between UAV and TLS methods in road cracks mapping to determine the location, types and measurements of road cracks as well as to practically test the feasibility of these techniques in identifying damaged pavement. The research outlines two objectives: (1) To test the feasibility of UAV and TLS technology in road cracks detection; and (2) To analyse the output between the UAV and

TLS in road cracks mapping. The findings from this study proposed provide detailed insight and contribution to the Malaysian Public Work Department (JKR) and other related agencies in road maintenance to locate the damaged pavements based on UAV and TLS technologies. It is important to identify the potential use of UAV and TLS to serve as a long-term alternative in providing typical road condition information. This paper begins by reviewing scholarly sources related to the topic to build a theoretical framework. Later, the methodology is stated starting from preliminary planning, data collection and analysis. Then, result and analysis is done carefully in a systematic way. This paper wraps up by emphasising the main idea and the findings of this study.

2. LITERATURE REVIEW

2.1 Overview of Road

Mahajan (2020) and Mohod et al. (2016) defined the road as a type of hard surface constructed from subgrade, sub-base, base course and surface course or wearing course. It is designed to handle the traffic loads and serve as a convenient travel surface for vehicles or pedestrians that grants resistance for transportation to provide a comfortable and safe travel path at the upper surface of natural soil. Road networks in Malaysia were developed and upgraded in response to the country's political and economic situation, notably through the Malaysia Plan launched by the Federal Government. In Malaysia, the JKR under the Ministry of Works (MOW) is responsible for road construction and maintenance.

The road condition refers to the factors describing the ease of driving on the road, including the quality of the pavement surface, potholes, road markings and weather. Pavement inhabits deteriorate negligent through time as a result of distresses over time. Major asphalt pavement surface distresses include cracking, surface deformation, disintegration and surface defects. However, the pavement lifespan can be extended for an estimated 20 to 40 years period with proper and regular maintenance and rehabilitation (Konvshenin, 2013). Besides, road condition is a key criterion in Pavement Management System (PMS), which aggregate and communicate data to make timely decisions on maintenance options for distressed pavements (Ruotoistenmäki & Seppälä, 2007).

2.1.1 Road Cracks Classification: Road cracks are fissures caused by complete or partial fractures of the pavement surface that come in different forms, which normally begin with a very tiny crack then widen and erode with age to an interconnected pattern over the entire pavement surface associated with cracks are loss of water proofing of the pavement layers, loss of load spreading ability, loss of fines from the base due to pumping, loss of riding quality and loss of appearance (Arizan, 2020). This issue is currently progressing at an alarming rate that is pressing the attention from both academic and industrial agencies as damaged pavements are considered one of the largest contributing factors to fatal motor vehicle crashes (Fares et al., 2010). In Distress Identification Manual for Long-Term

Pavement Performance project (SHRP-P-338, 1993), cracks for asphalt concrete pavement can be categorised into six types as shown in Figure 1 and Table 1.

Table 1 describes the characteristics of each type of road crack (JKR, 1992). There are three severity levels for each type, namely low, moderate and high.

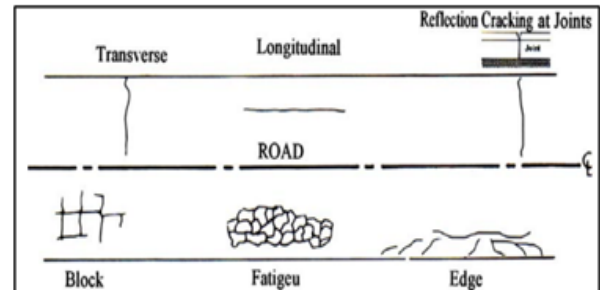


Figure 1. Types of Road Cracks (JKR, 1992)

| Types | Description |
|-----------------------------------|---|
| Fatigue Crack / Alligator Crack | A pattern of interconnected cracks in the initial stage of growth due to brittle base and inadequate pavement thickness. Ultimately, the surface develops multiple sides and sharp-angled fragments. |
| Longitudinal Crack / Linear Crack | Refers to crack that run parallel to the centerline of the pavement, which is resulted from poor paving lane joint, fatigue failure of asphalt concrete, reflective cracking and cut-fill differential settlement. |
| Transverse Crack | Described as those cracks that is perpendicular to the centerline of the pavement due to the reflection of shrinkage cracking and construction joints. |
| Block Crack | Large rectangle pieces of crack pattern that ranges in size approximately within 0.1 m ² to 10 m ² . |
| Edge Crack | Crescent-shaped cracks that intersect the pavement edge and are located within 0.6 m of the pavement edge. Pavements with unpaved shoulders are susceptible to edge cracking. Edge crack is due to inadequate pavement width and edge support, traffic travelling on shoulder edge drop and loss of adhesion. |
| Joint Reflection Crack | Describes the fractures in bitumen overlay surface that appear over the concrete pavement joints which caused by the movement of cement concrete slab under road surface due to thermal and moisture changes. |

Table 1. Characteristics of Road Cracks Categories

2.2 Photogrammetry

Photogrammetry is a technique to obtain reliable information about physical objects and their surroundings by capturing, measuring and interpreting images and digital representations of

energy patterns produced by non-contact sensor devices (Wolf & Dewitt, 2000). Based on triangulation principle, the photogrammetry establishes geometric relationship between two-dimensional (2D) image of an object and three dimensional (3D) spaces coordinates at the instant when the image is captured. Triangulation is generated by taking images from various positions and the intersection of "lines of sight" from the camera to points on an object.

Photogrammetry based on the data acquisition system is divided into terrestrial and aerial photogrammetry. Aerial photogrammetry involves the acquisition of photographs of the earth surface or terrain of an area using an aerial camera fixed beneath the aircraft body. Multiple overlapping photos were taken and aerial triangulation is employed to produce sufficient points for the photogrammetric model from GCP. In contrast, terrestrial photogrammetry is a method where the camera is mounted on a tripod or vehicle to take the photographs from a fixed and known position on or near the ground. It is commonly used at ground level for small-scale surveying, manufacturing and industrial applications.

2.3 Terrestrial Laser Scanning (TLS)

TLS is ground-based light detection and ranging (LiDAR) system and it is an industrial-grade surveying device. It uses the laser technology to measure everything in the laser field of view, whereby continuous eye-safe laser beam is emitted rapidly while the laser scanner will automatically rotate at 360° horizontally and 300° vertically to observe thousands of points within seconds. The spinning of mirrors allows laser beam up and down results in systematic sweeping of laser beam. In conjunction with the backscattered energy bounces back to the laser scanner, it enables the system to record the corresponding horizontal angle of the rotating laser and the subsequent vertical angle of the moving mirror. This survey approach requires the target to be scanned from different standpoints to register single point cloud to a common point cloud and finally generates a digital representation of scene, known as dense point cloud, which comprises of coordinates data (x,y,z) in 3D space and intensity values for each point.

2.4 Unmanned Aerial Vehicle (UAV)

UAV or known as drone is a small aircraft that fly without an onboard pilot that fly by aerodynamic lift UAV system and typically equipped with a digital camera or video recorder. Its flight is controlled either autonomously by onboard computers or by the remote control of a pilot on the ground or in another vehicle. UAV photogrammetry is faster, closer and cheaper in traffic monitoring compared with satellite monitoring.

Flight planning in aerial photogrammetry helps to ensure all necessary data is collected. According to Tahar (2013), flight planning entails the location of control points for the photographs and the placement of flight lines on a map of the required area. Flight plans are composed of a flight map and

specification, with the flight map defining the project's borders and flight lines across the desired coverage area.

While flight altitude is important in UAV mapping since it determines the covered area, pixel size on the registered images and flight duration. Mesas-Carrascosa et al. (2016) concluded that lower altitude flights and the use of GCPs give better absolute positional accuracy. It indicates that flight altitude has a direct impact on the errors produced. Research with UAV based photogrammetric technique done by Zulkipli and Tahar (2018) clearly shows that UAV with flight at low altitude are capable of road mapping. Hence, it can be concluded that low altitude during flight planning is most probably suitable to map the road condition.

2.5 Digital Terrain Model (DTM)

DTM is one of the methods used to represent earth surface of an area. According to the sampling method, it comprises of coordinated points X, Y and Z. DTM data can be obtained with remote sensing and land surveying techniques. It is a vector data set used to represent the ground surface landform in topographic maps and define the position by latitude, longitude and terrain elevation. DTM was introduced in 1958 by Millerand and Laflamme to expedite highway design by digital computation based on photogrammetrically acquired terrain data (Doyle, 1978). In short, DTM only gives the interpretation of bare earth model which can be obtained from further process of a digital surface model (DSM).

2.6 Accuracy Assessment

Root Mean Square Error (RMSE) is commonly accepted statistical measurement used to assess output accuracy which helps to measure the differences between values predicted and values being observed. As shown below is the formula for RMSE.

$$RMSE = \pm \sqrt{\frac{\sum_{i=1}^n (\text{Observed data} - \text{Reference or Actual data})^2}{N}} \quad (1)$$

In this study, the UAV and TLS observed data were compared with actual data to check and compare their accuracy.

2.7 Related Research

The topics related to road conditions in term of pavement distress have been studied few years ago. Kubota et al. (2020) in Japan discovered that 3D data derived from the fusion of TLS and UAV aids the road maintenance system. In Turkey, Zeybek and Biçici (2020) performed road distress measurements using UAV and they concluded that both results from UAV and traditional inspection are pretty similar. According to the findings of Garba (2017) in Malaysia, the author mentioned that TLS has potential in the data collection for road management system. The research gap has been investigated and it was found that no previous research had been conducted in Malaysia to compare the assessment of road cracks mapping using UAV and TLS.

3. METHODOLOGY

The research methodology comprises of 4 phases as shown in Figure 2.

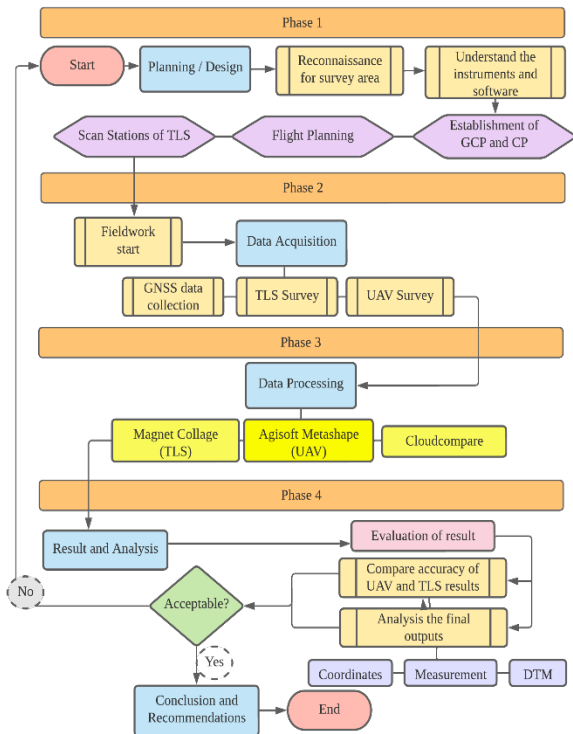


Figure 2. Flow Chart of Methodology

3.1 Planning

In Phase 1, focus is given to the progress planning of this study that comprises of an extensive review of past literatures, the identification and design of the survey area. The selected study areas are in the campus of Universiti Teknologi Malaysia (UTM), Skudai, Johor Bahru where the first study area is the road located near the UTMSpace and the second study area is the road at block XB 2 Kolej Dato' Onn Jafar (KDOJ), UTM. Besides, the strategy plan of UAV flight planning with Drone Deploy software, scan stations for TLS and establishment of GCPs and CPs in study areas were pre-planned carefully.

3.2 Data Acquisition

In this study, there are three types of data obtained, including the GNSS data, aerial image data and TLS dense data. Firstly, static and rapid-static methods were applied for GNSS data collection at GCPs and CPs respectively using Topcon Hiper-HR receivers. After post-processing the GNSS data, this greatly helps to increase the accuracy for next data collection when GCPs and CPs were established with known coordinates. Then, low altitude aerial imagery was collected using the DJI Phantom 4 over the road surface. Later, TLS data collection using Topcon GLS-2000 was set-up properly at the pre-planned routes of GCPs and CPs

to obtain the dense data of road. TLS was implemented using traversing method where it comprises a backsight and foresight station such that each TLS can scan the road's features from the ground.

3.3 Data Processing

Phase 3 is mainly on the data processing using suitable software. In this phase, the road data obtained were processed and split into three main components: GCPs and CPs data processing, UAV data processing and TLS point clouds processing. Raw GNSS observation data was processed via tps2rin.exe and Trimble Business Centre (TBC) software with connection to the MyRTKnet and ISKnet. Later, the Agisoft Metashape was used for aerial data processing whereas the TLS data was processed by the Magnet Collage and CloudCompare software. The coordinates of the control points, measurements and types of road cracks were recorded in table form. Later, those unnecessary point clouds of road data from UAV and TLS were filtered and cleaned to generate the DTM.

3.4 Data Analysis

The last phase involves presenting the outputs in a systematic way and clarifying the analysis to evaluate the feasibility of the techniques used in road cracks mapping. From the UAV and TLS data obtained, the coordinates of control points, types and measurements of road cracks and the DTMs were analysed. Then, the accuracy assessment in form of RMSE was computed. The results were evaluated with the reference data where a standard measuring tape was used to verify the road crack measurements while the GNSS data was employed to check the coordinates of control stations obtained by UAV and TLS.

4. RESULTS AND DISCUSSION

4.1 Output of UAV

The high-quality dense point cloud is set in Agisoft Metashape with eight GCPs were employed for georeferencing purposes. The software can generate products such as orthomosaic, digital terrain model, densified point cloud and 3D textured mesh as shown in Figure 3 and Figure 4.



Figure 3. Orthophotos for Study Area 1 (Left) and Study Area 2 (Right)

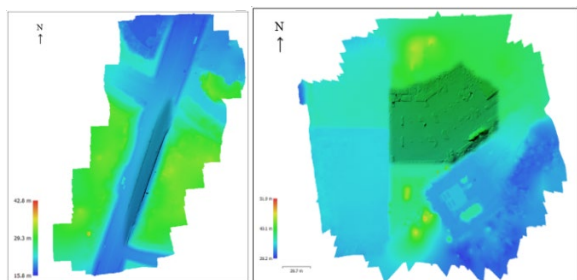


Figure 4. DTM for Study Area 1 (Left) and Study Area 2 (Right)

4.2 Output of TLS

The raw point clouds were registered, merged and georeferenced to produce complete point cloud model as shown in Figure 5. GLS-2000 is a long-range scanner hence unnecessary point cloud is then cleaned in Magnet Collage. Then, the types and measurement of the road cracks were observed. Later, the point cloud was exported into *.las format and undergo DTM processing in CloudCompare.

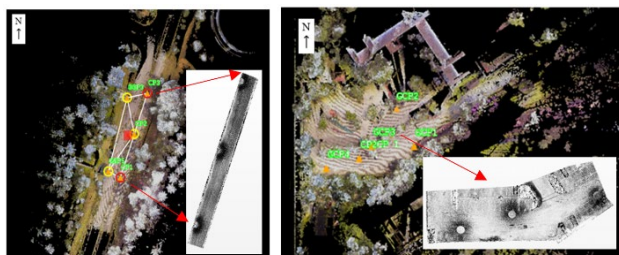


Figure 5. TLS Point Clouds Model for Study Area 1 (Left) and Study Area 2 (Right)

4.3 Qualitative Analysis

4.3.1 Point Cloud: Based on the point cloud within UAV and TLS, it obviously shows that UAV has a bigger coverage area than TLS. The TLS only able to scan the objects visible in the line-of-sight, which brings the effects that TLS captured the passing vehicles during data collection. However, in terms of point cloud density, TLS has a denser point cloud compared to UAV, leading in better visualization, positioning and others. Moreover, TLS point cloud data has a higher intensity level than UAV point cloud data where TLS has 17,937,241 and 14,565,567 intensity values while UAV has 424,483 and 695,920 intensity values for study area 1 and study area 2 respectively.

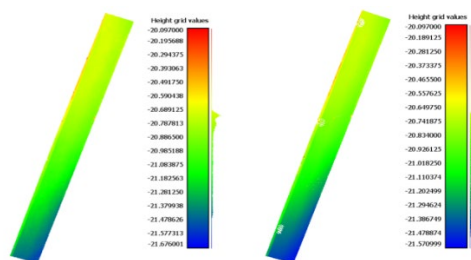


Figure 6. Height Grid Values for UAV (Left) and TLS (Right) in Colour Scale Mode for Study Area 1

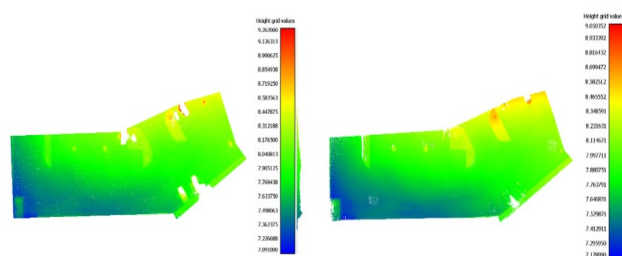


Figure 7. Height Grid Values for UAV (Left) and TLS (Right) in Colour Scale Mode for Study Area 2

In order to have a clearer view, cloud-to-cloud (C2C) distance method was employed to compare the cloud distances within the DTM rasters from UAV and TLS. Ahmad et al. (2018) have asserted that the best option for comparing two datasets of point clouds is least square plane method. Hence, the derived DTMs model from both approaches were compared with each other.

A high degree of compatibility between the DTM UAV and TLS is shown in Figure 8, which present the analysis results of C2C for each study area, with a difference mean distance lower than 2 centimeters (cm) between both models. This finding is supported by Mitika et al. (2018) where they generate quite a similar result in range of cm level in their comparative study of terrain model generation using UAV and TLS

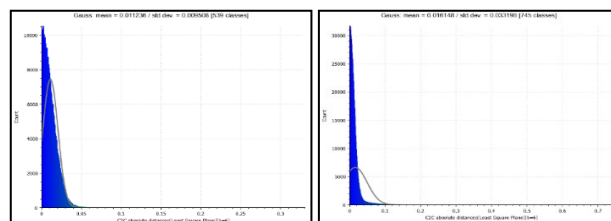


Figure 8. Graphs of C2C Absolute Distance for DTM Raster Study Area 1(left) and 2 (right)

4.4 Quantitative Analysis

The quantitative analysis mainly covered the control points and the road cracks measurement generated by UAV and TLS. The quality assessments of both approaches were done by RMSE calculations.

4.4.1 Coordinates of Control Points: Table 2 and Table 3 show the comparison of the control points from UAV and TLS data that were evaluated by GNSS coordinates for both study areas.

| Points | UAV | | | GNSS | | | Differences | | | |
|--------|-------------|--------------|---------------|-------------|--------------|---------------|--------------|--------------|---------------|---------|
| | Easting (m) | Northing (m) | Elevation (m) | Easting (m) | Northing (m) | Elevation (m) | Easting (m) | Northing (m) | Elevation (m) | |
| CP 1 | 628655.611 | 172620.897 | 20.591 | 628655.599 | 172620.926 | 20.578 | 0.012 | -0.029 | 0.013 | |
| CP 2 | 628667.381 | 172656.340 | 21.043 | 628667.403 | 172656.337 | 21.034 | -0.022 | 0.003 | 0.009 | |
| CP 3 | 628678.581 | 172689.459 | 21.195 | 628678.570 | 172689.458 | 21.175 | 0.011 | 0.001 | 0.020 | |
| CP 1 | 624561.956 | 174149.674 | 37.099 | 624561.895 | 174149.642 | 37.178 | 0.061 | 0.032 | -0.079 | |
| CP 2 | 624551.965 | 174149.420 | 37.128 | 624551.922 | 174149.424 | 37.166 | 0.043 | -0.004 | -0.038 | |
| CP 3 | 624541.807 | 174149.329 | 37.057 | 624541.808 | 174149.329 | 37.088 | -0.001 | 0.000 | -0.031 | |
| | | | | | | | RMSE | ± 0.032 | ± 0.018 | ± 0.039 |
| | | | | | | | Average RMSE | ± 0.030 m | | |

Table 2. Accuracy Assessment of Check Points for UAV data

| Points | TLS | | | GNSS | | | Differences | | | |
|--------|-------------|--------------|---------------|-------------|--------------|---------------|--------------|--------------|---------------|---------|
| | Easting (m) | Northing (m) | Elevation (m) | Easting (m) | Northing (m) | Elevation (m) | Easting (m) | Northing (m) | Elevation (m) | |
| GCP 3 | 628661.297 | 172685.791 | 20.874 | 628661.297 | 172685.791 | 20.875 | 0 | 0 | -0.001 | |
| GCP 5 | 628645.219 | 172625.966 | 20.369 | 628645.219 | 172625.966 | 20.37 | 0 | 0 | -0.001 | |
| CP 1 | 628655.599 | 172620.926 | 20.578 | 628655.599 | 172620.926 | 20.578 | 0 | 0 | 0 | |
| GCP 1 | 624585.139 | 174156.578 | 37.402 | 624585.139 | 174156.578 | 37.402 | 0 | 0 | 0 | |
| GCP 2 | 624573.652 | 174178.725 | 38.168 | 624573.652 | 174178.725 | 38.168 | 0 | 0 | 0 | |
| GCP 3 | 624559.652 | 174157.029 | 37.54 | 624559.658 | 174157.034 | 37.54 | -0.006 | -0.005 | 0 | |
| GCP 4 | 624531.953 | 174143.506 | 36.774 | 624531.97 | 174143.509 | 36.775 | -0.017 | -0.003 | -0.001 | |
| | | | | | | | RMSE | ± 0.007 | ± 0.002 | ± 0.001 |
| | | | | | | | Average RMSE | ± 0.003 m | | |

Table 3. Accuracy Assessment of Selected Control Points for TLS Data

The average RMSE value for the accuracy assessment of selected control points for TLS data is only ± 0.003 m which is lower than UAV data that yields ± 0.030 m. This indicates that TLS is more reliable compared to UAV method in terms of positioning or mapping due to TLS is a ground-based active system.

4.4.2 Road Cracks Measurement: Based on Figure 9 to Figure 12, there were several types of road cracks can be found. The road cracks measurement obtained from UAV and TLS data were measured by specific software and was evaluated by manual inspection method.

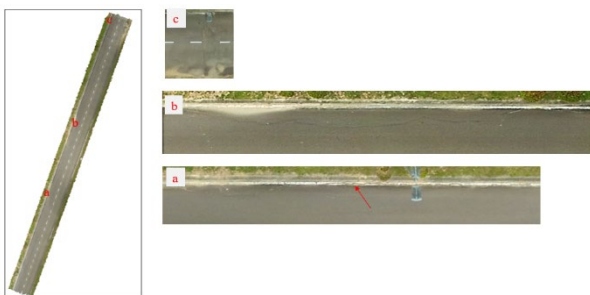


Figure 9. Detection of Road Cracks from UAV data for Study Area 1

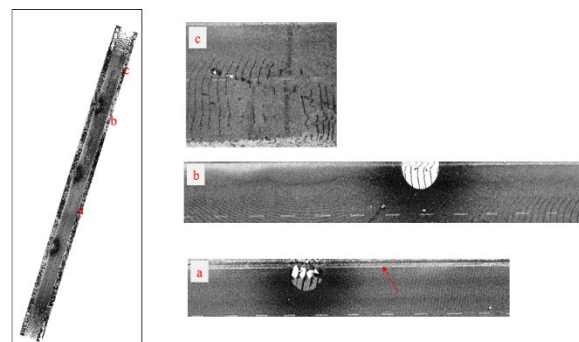


Figure 10. Detection of Road Cracks from TLS Data for Study Area 1



Figure 11. Detection of Road Cracks from UAV Data for Study Area 2

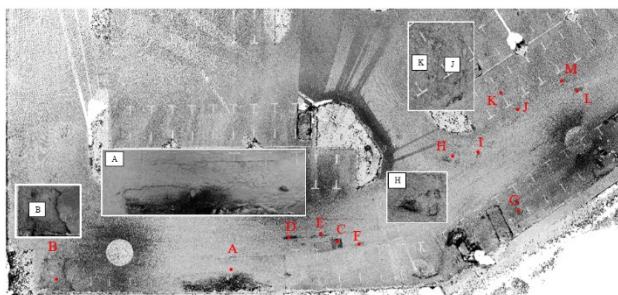


Figure 12. Road Cracks Detection from TLS Data in Study Area 2

Using road crack A in Figure 14 from UAV data and in Figure 15 from TLS data as an example, the measurement taken was verified with field measurement with a measuring tape as shown in Figure 13. Table 4 shows the accuracy assessment of road cracks measurement based on UAV data while Table 5 shows accuracy assessment of road cracks measurement based on TLS data.

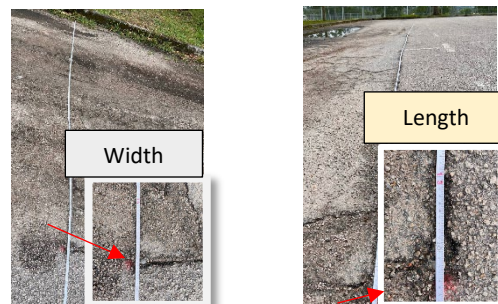


Figure 13. Manual Evaluation by Measuring Tape for Crack A

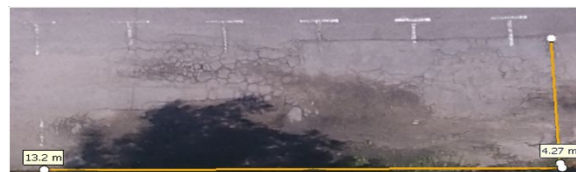


Figure 14. Crack A From UAV Data In Agisoft Metashape



Figure 15. Crack A taken from TLS data in Magnet Collage

| Cracks | Types | UAV | | | MANUAL | | | Differences UAV-Manual | | |
|--------|------------------------|------------|-----------|------------------------|------------|-----------|------------------------|------------------------|-----------|------------------------|
| | | Length (m) | Width (m) | Area (m ²) | Length (m) | Width (m) | Area (m ²) | Length (m) | Width (m) | Area (m ²) |
| a | Edge | 11.600 | 0.032 | 0.371 | 11.507 | 0.041 | 0.472 | 0.093 | -0.009 | -0.101 |
| b | Edge | 24.800 | 1.300 | 32.240 | 24.000 | 1.405 | 33.720 | 0.800 | -0.105 | -1.480 |
| c | joint reflection crack | 7.130 | 1.290 | 9.198 | 7.060 | 1.201 | 8.479 | 0.070 | 0.089 | 0.719 |
| A | Fatigue | 13.200 | 4.250 | 56.100 | 13.128 | 4.216 | 55.348 | 0.072 | 0.034 | 0.752 |
| B | Fatigue | 4.840 | 4.680 | 22.651 | 4.845 | 4.720 | 22.868 | -0.005 | -0.040 | -0.217 |
| C | Block | 3.140 | 1.030 | 3.234 | 3.160 | 1.200 | 3.792 | -0.020 | -0.170 | -0.558 |
| D | Longitudinal | 2.200 | 0.282 | 0.620 | 2.760 | 0.260 | 0.718 | -0.560 | 0.022 | -0.097 |
| E | Longitudinal | 4.790 | 0.291 | 1.394 | 4.960 | 0.210 | 1.042 | -0.170 | 0.081 | 0.352 |
| F | Fatigue | 1.760 | 0.566 | 0.996 | 1.870 | 0.553 | 1.034 | -0.110 | 0.013 | -0.038 |
| G | Pothole | 1.020 | 0.496 | 0.506 | 1.890 | 0.260 | 0.491 | -0.870 | 0.236 | 0.015 |
| H | Fatigue + pothole | 2.870 | 1.490 | 4.276 | 2.760 | 1.750 | 4.830 | 0.110 | -0.260 | -0.554 |
| I | Pothole | 3.150 | 2.310 | 7.277 | 3.139 | 2.228 | 6.994 | 0.011 | 0.082 | 0.283 |
| J | Pothole | 5.150 | 0.443 | 2.281 | 5.035 | 0.437 | 2.200 | 0.115 | 0.006 | 0.081 |
| K | Pothole | 5.570 | 1.180 | 6.573 | 5.543 | 1.175 | 6.513 | 0.027 | 0.005 | 0.060 |
| L | Pothole | 0.715 | 0.154 | 0.110 | 0.725 | 0.168 | 0.122 | -0.010 | -0.014 | -0.012 |
| M | Pothole | 0.969 | 0.392 | 0.380 | 1.079 | 0.296 | 0.319 | -0.110 | 0.096 | 0.060 |
| | | | | | | | RMSE | ± 0.336 | ± 0.111 | ± 0.511 |
| | | | | | | | Average RMSE | ± 0.224 m | | |

Table 4. Accuracy assessment of road cracks measurement based on UAV data

| Cracks | Types | TLS | | | MANUAL | | | Differences TLS-Manual | | |
|--------|------------------------|------------|-----------|------------------------|------------|-----------|------------------------|------------------------|-----------|------------------------|
| | | Length (m) | Width (m) | Area (m ²) | Length (m) | Width (m) | Area (m ²) | Length (m) | Width (m) | Area (m ²) |
| a | Edge | 11.538 | 0.043 | 0.496 | 11.507 | 0.041 | 0.472 | 0.031 | 0.002 | 0.024 |
| b | Edge | 24.013 | 1.434 | 34.435 | 24.000 | 1.405 | 33.720 | 0.013 | 0.029 | 0.715 |
| c | joint reflection crack | 7.024 | 1.198 | 8.415 | 7.060 | 1.201 | 8.479 | -0.036 | -0.003 | -0.064 |
| A | Fatigue | 13.131 | 4.195 | 55.085 | 13.128 | 4.216 | 55.348 | 0.003 | -0.021 | -0.263 |
| B | Fatigue | 4.847 | 4.740 | 22.975 | 4.845 | 4.720 | 22.868 | 0.002 | 0.020 | 0.106 |
| C | Block | 3.215 | 1.224 | 3.935 | 3.160 | 1.200 | 3.792 | 0.055 | 0.024 | 0.143 |
| D | Longitudinal | 2.834 | 0.351 | 0.995 | 2.760 | 0.260 | 0.718 | 0.074 | 0.091 | 0.277 |
| E | Longitudinal | 5.060 | 0.243 | 1.230 | 4.960 | 0.210 | 1.042 | 0.100 | 0.033 | 0.188 |
| F | Fatigue | 1.994 | 0.570 | 1.137 | 1.870 | 0.553 | 1.034 | 0.124 | 0.017 | 0.102 |
| G | Pothole | 1.997 | 0.267 | 0.533 | 1.890 | 0.260 | 0.491 | 0.107 | 0.007 | 0.042 |
| H | Fatigue + pothole | 2.735 | 1.789 | 4.893 | 2.760 | 1.750 | 4.830 | -0.025 | 0.039 | 0.063 |
| I | Pothole | 3.128 | 2.224 | 6.957 | 3.139 | 2.228 | 6.994 | -0.011 | -0.004 | -0.037 |
| J | Pothole | 5.015 | 0.425 | 2.131 | 5.035 | 0.437 | 2.200 | -0.020 | -0.012 | -0.069 |
| K | Pothole | 5.533 | 1.171 | 6.479 | 5.543 | 1.175 | 6.513 | -0.010 | -0.004 | -0.034 |
| L | Pothole | 0.734 | 0.176 | 0.129 | 0.725 | 0.168 | 0.122 | 0.009 | 0.008 | 0.007 |
| M | Pothole | 0.983 | 0.408 | 0.401 | 0.976 | 0.400 | 0.390 | 0.007 | 0.008 | 0.011 |
| | | | | | | | RMSE | ± 0.055 | ± 0.029 | ± 0.217 |
| | | | | | | | Average RMSE | ± 0.042 m | | |

Table 5. Accuracy assessment of road cracks measurement based on TLS data

It was found that TLS and UAV yield quite similar results when comparing the accuracy assessment in terms of measurement for both approaches to the reference data from manual inspection. The accuracy of TLS obtained values was supported by low differences between TLS and field measurement while UAV-derived result shows weaker performance.

This is due to the fact that point cloud of TLS is a direct result of measurement as opposed to UAV technology which are derivatives from the imagery obtained (Wójcik et al., 2019). As shown in Figure 16 is the box-and-whisker plot for average differences obtained from the results

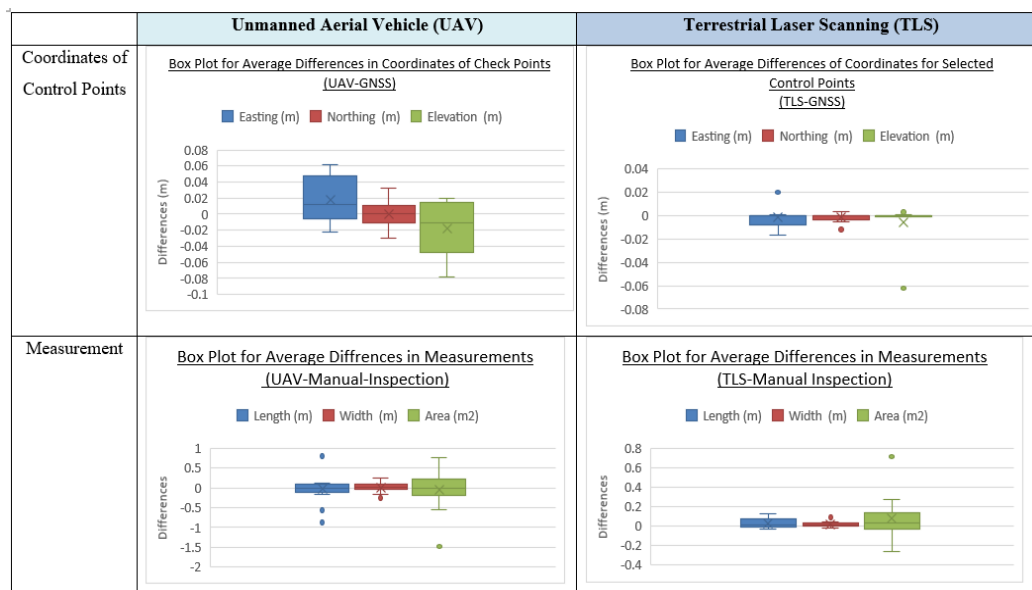


Figure 16. Box-and-whisker plot for average differences of results obtained

5. DISCUSSION

Understand that both approaches are feasible in road cracks mapping, hence the identification of the advantages and disadvantages based on different views within UAV and TLS are discussed in Table 6 and 7.

| UAV | |
|---------------|---|
| Advantages | <ul style="list-style-type: none"> • Cost-effective • Time-saving • Lightweight • The operator is not required to be in close proximity to the object being measured • Ability to perform measurements in hazardous or inaccessible areas. |
| Disadvantages | <ul style="list-style-type: none"> • Weather dependent • Analyzing point clouds does not constitute original measurements but is derived from the aerial imagery. • Centimeter range accuracy |

Table 6. Strengths and Weaknesses of UAV in Road Cracks Mapping

| TLS | |
|---------------|---|
| Advantages | <ul style="list-style-type: none"> • High spatial data for analysis purposes • Unlimited use of point cloud for further generation • The point obtained consists of real X, Y and Z coordinates of the object • Robust against poor weather • High accuracy. |
| Disadvantages | <ul style="list-style-type: none"> • Limited field of view for scanner • High-cost and time consuming due to several scan stations • Heavier and become more difficult to be carried when area is not accessible • TLS method as not as safe as using UAV. Operator needs to be in close proximity to the object being measured |

Table 7. Strengths and Weaknesses of TLS in Road Cracks Mapping

6. CONCLUSION

The UAV-based photogrammetry and TLS present the differences in terms of data acquisition modes, typical project sizes, scanning mechanisms, resolution and accuracy capabilities. This study has successfully achieved the aim and objectives as well as provides a broad overview of their performance and the potential use of UAV and TLS for road cracks mapping. The comparative analysis successfully performed and both methods yield quite similar results in terms of positioning and measurement, which were evaluated using GNSS and manual inspection respectively, with the average RMSE differences ranging from ± 0.003 m to ± 0.030 m for coordinates errors and ± 0.042 m to ± 0.224 m for measurement error. However, the results highlighted that TLS poses higher

accuracy than UAV in terms of the position of control points and road cracks measurement. Meanwhile, there are minor differences in DTM quality at the centimetre level between these methods. Owing to the findings, it can be concluded that TLS with lidar technology is more reliable and accurate than UAV in mapping and measuring work. However, depending on several factors including costs, time, safety and accessibility, UAV provides the decisive advantages compare to TLS. In short, UAV is more practical used than TLS method, but in terms of accuracy TLS yields a better performance than UAV. It is hoped that this work contributes to existing knowledge of road cracks mapping by providing the insights of using modern technology.

Understanding that lidar technology is useful in producing fast and high-quality result, hence further research on this topic is necessary. As UAV is more suitable to be employed in hazardous environment, while mobile laser scanning can quickly response to the ground condition. It is recommended that the assessment for road condition mapping using neither UAV lidar Phantom RTK nor mobile laser scanning methods can be investigated in future.

ACKNOWLEDGEMENT

The authors wish to extend their appreciation to UTM research grant no Q.J130000.4352.09G75 for sponsoring this study and making it successful. Special thanks to Faculty Built Environment & Surveying, UTM for supporting this work by providing instruments and information for data collection and eventually fulfil the part of result and analysis for this work.

REFERENCES

- Ahmad Fuad, N., Yusoff, A. R., Ismail, Z., & Majid, Z. (2018). *Comparing The Performance Of Point Cloud Registration Methods For Landslide Monitoring Using Mobile Laser Scanning Data*. ISPRS - International Archives of the Photogrammetry, Remote Sensing and Spatial Information Sciences, XLII4/W9, 11–21. <https://doi.org/10.5194/isprs-archives-xlii-4-w9-11-201>
- Ahmad Ramly (2002). *Prinsip dan Praktis Pengurusan Penyelenggaraan Bangunan*. Pustaka Ilmi, Selangor
- Alsadik, B., & Remondino, F. (2020). *Flight planning for LiDAR-based UAS mapping applications*. ISPRS international journal of geo-information, 9(6), 378.
- Doyle, F., Mikhail, E. M., Ackermann, F., Mikhail, E., Jancaitis, J., Helava, U., ... & Helmering, R. (1978). *PANEL DISCUSSION-FUTURE OF DTM*. Photogrammetric Engineering and Remote Sensing, 44(12), 1487-1497.
- Fares H, Shahata K, Elwakil E et al. (2010) *Modelling the performance of pavement marking in cold weather conditions*. Structure and Infrastructure Engineering 8(11): 1067–1079

- Firdausi Musa Garba. (2017). *Road Conditional Mapping Using Terrestrial Laser Scanning Method*. Universiti Teknologi Malaysia.
- Idris, A. R., & Mohamed, I. S. (2020). *Jalan rosak undang maut*. Utusan Digital. <https://www.utusan.com.my/berita/2020/12/jalan-rosak-undang-maut/?msclkid=4161bd02b0cd11ecbf5a576f189b9b9e>
- Jabatan Kerja Raya Malaysia. (1992). *A Guide to Visual Assessment of Flexible Pavement Surface Conditions*. Malaysia: Jabatan Kerja Raya Malaysia
- Jabatan Kerja Raya Malaysia. Bahagian Senggara Fasiliti Jalan. (2021). *STATISTIK JALAN MALAYSIA EDISI 2021*. Jabatan Kerja Raya Malaysia, Bahagian Senggara Fasiliti Jalan. <https://www.jkr.gov.my/my/page/dokumen-teknikal-0>
- Khairy Jamaluddin. (2020). Khairy injured in fall while cycling. Twitter. <https://www.thestar.com.my/news/nation/2020/12/27/khairy-injured-in-fall-while-cycling?msclkid=54de0fedb31811ecb00103f7454c5a42>
- Konvshenin, K. (2013). *Long-Life Pavements* | PRRCenter. Pavement Recycling and Reclaiming Center (PRRC); California State Polytechnic University, Civil Engineering Department. http://prrcenter.org/?page_id=92
- Kubota, S., Hata, R., Nishi, K., Ho, C., and Yasumuro, Y. (2020). *Road Maintenance Management System Using 3D Data by Terrestrial Laser Scanner and UAV*. ISARC Proceedings, 1337–1343. http://www.iaarc.org/publications/2020_proceedings_of_the_37th_isarc/road_maintenance_management_system_using_3d_data_by_terrestrial_laser_scanner_and_uav.html
- Leonardi, G., Barrile, V., Palamara, R., Suraci, F., & Candela, G. (2018). *3D Mapping of Pavement Distresses Using an Unmanned Aerial Vehicle (UAV) System*. New Metropolitan Perspectives, 164–171. https://doi.org/10.1007/978-3-319-92102-0_18
- Mahajan, B. (2020). *What Is Pavement - Types Of Pavement*.pdf. <https://civiconcepts.com/blog/what-is-pavement-types-of-pavement-road-construction-layers>
- Mesas-Carrascosa, F. J., Notario García, M. D., Meroño de Larriva, J. E., & García-Ferrer, A. (2016). *An analysis of the influence of flight parameters in the generation of unmanned aerial vehicle (UAV) orthomosaics to survey archaeological areas*. Sensors, 16(11), 1838.
- Mitka, B., Klapa, P., & Piech, I. (2018). Comparative analysis of geospatial data received by TLS and UAV technologies for the quarry. International Multidisciplinary Scientific GeoConference: SGEM, 18(2.3), 57-64.
- Miraliakbari, A., Hahn, M., & Maas, H. G. (2014). *Development Of A Multi-Sensor System For Road Condition Mapping*. International Archives of the Photogrammetry, Remote Sensing & Spatial Information Sciences.
- Mohd Arizanfa bin Mokhtar. (2020). *Road Damage And Maintenance Along Federal Road In Kuala Krai, Kelantan*. Doctoral dissertation, Universiti Teknologi Malaysia.
- Mohod, M. V., & Kadam, K. N. (2016). *A comparative study on rigid and flexible pavement: a review*. IOSR Journal of Mechanical and Civil Engineering (IOSR-JMCE), 13(3), 84-8
- Okal, M. (2017). *TLS Parameters, Workflows and Field Methods*. https://kb.unavco.org/kb/assets/807/SGTF_TLSShortCourse_MHO.pdf
- Ruotoistenmäki, A., & Seppälä, T. (2007). *Road condition rating based on factor analysis of road condition measurements*. Transport Policy, 14(5), 410-420. <https://doi.org/10.1016/j.tranpol.2007.03.006>
- Salleh, N. F. (2016). *Jalan Rosak, Berlubang Jadi Punca Kemalangan Maut*. MediaKota. <https://mediatvkota.wordpress.com/2016/12/25/jalan-rosak-berlubang-jadi-punca-kemalangan-maut/?msclkid=4161f387b0cd11ec89163e869bf9abcb>
- SHRP-P-338, National Research Council. (1993). *Distress identification manual for the long-term pavement performance project*. Strategic Highway Research Program, USA regulation, Washington, DC, Available at <http://onlinepubs.trb.org/onlinepubs/shrp/shrp-p-338.pdf>.
- Staniek, M. (2017). *Detection of cracks in asphalt pavement during road inspection processes*. Zeszyty Naukowe. Transport/Politechnika Śląska.
- Tahar, K. N. (2013). *An evaluation on different number of ground control points in unmanned aerial vehicle photogrammetric block*. Int. Arch. Photogramm. Remote Sens. Spat. Inf. Sci, 40, 93-98.
- Wang, Q., Tan, Y., & Mei, Z. (2019). *Computational Methods of Acquisition and Processing of 3D Point Cloud Data for Construction Applications*. Archives of Computational Methods in Engineering, 27(2), 479-499. <https://doi.org/10.1007/s11831-019-09320-4>
- Wartawan Nabalu News. (2021). *Jalan rosak, berlubang antara punca kemalangan Telupid-Sandakan*. *Jalan rosak, berlubang antara punca kemalangan Telupid-Sandakan*. <https://www.nabalunews.com/post/jalan-rosak-berlubang-antara-punca-kemalangan-sandakan-telupid?msclkid=416321fdb0cd11ecb74bded78abd18e3>
- Wójcik, A., Klapa, P., Mitka, B., & Piech, I. (2019). The use of TLS and UAV methods for measurement of the repose angle of granular materials in terrain conditions. Measurement, 146, 780–791. <https://doi.org/10.1016/j.measurement.2019.07.015>
- Wolf, P. R., Dewitt, B. A., & Wilkinson, B. E. (2014). *Elements of Photogrammetry with Applications in GIS*. McGraw-Hill Education.

Yurtseven, H. (2019). *Comparison of GNSS-, TLS- and Different Altitude UAV-Generated Datasets on The Basis of Spatial Differences*. ISPRS International Journal of Geo-Information, 8(4). <https://doi.org/10.3390/ijgi8040175>

Zeybek, M., & Biçici, S. (2020). *Road distress measurements using UAV*. Turkish Journal of Remote Sensing and GIS, 1(1), 13-23.

Zhang, C. (2008). *An UAV-based photogrammetric mapping system for road condition assessment*. Int. Arch. Photogramm. Remote Sens. Spatial Inf. Sci, 37, 627-632.

Zulkipli, M. A., & Tahar, K. N. (2018). *Multirotor UAV-based photogrammetric mapping for road design*. International Journal of Optics, 2018.